

Received: 16 December 2021 / Accepted: 25 March 2022 / Published online: 05 April 2022

*misalignment, FFT analysis,  
linear feed axis, motor current*

Mustafa DEMETGÜL<sup>1\*</sup>, Minjie GU<sup>1</sup>,  
Jonas HILLENBRAND<sup>1</sup>, Yicheng ZHAO<sup>1</sup>,  
Philipp GÖNNHEIMER<sup>1</sup>, Jürgen FLEISCHER<sup>1</sup>

## **MISALIGNMENT DETECTION ON LINEAR FEED AXIS WITH FFT AND STATISTICAL ANALYSIS USING MOTOR CURRENT**

The linear feed axes are critical subsystems in many production machines and have important responsibilities such as transporting workpieces and tools in the process. Therefore, the component's working condition is crucial for the production of high-quality products. Because these systems gradually deteriorate, it is necessary to detect these changes and occurring faults with condition monitoring systems. In this study, the motor current of feed axes is monitored for axis misalignment that occurs during or after assembly. We conduct diagnosis with Fast Fourier Transform (FFT) and statistical methods in order to differentiate different misalignment scenarios and operating constraints of the feed axis. Different states are achieved by simulating left and right axis misalignment and operating the table at different speeds and strokes.

### **1. INTRODUCTION**

One of the most important parts of Industry 4.0 is the acceleration of the transformation into unmanned factories by monitoring the machines remotely. A key enabler for this is suitable and robust condition monitoring (CM) systems, that act on the real-time data of machines [1–3]. These CM systems require a large number of sensors. Generally, fault detection and monitoring are performed by using acceleration sensors and vibration analysis [4], resulting in an additional cost for the machinery. In addition, these sensors are affected by environmental conditions and noise. Also, there are many parts of the machines that need to be monitored. This makes machine monitoring complex. This needs to be simplified. It is important to find many problems by monitoring only one piece of data on the machine. Using already available data sources of the machine can save expenses and installation efforts.

For this reason, in recent years, research and attempts have been made to use the motor current data of variable frequency drives (VFD) to diagnose machine faults. This method has many advantages compared with vibration, sound, acoustics, thermal, and other monitoring methods. Many machines have current monitoring for control and protection already installed, ensuring this monitoring technology is available on a vast number of machines.

---

<sup>1</sup> Institute of Production Science, Karlsruhe Institute of Technology, Germany

\* E-mail: mustafa.demetguel@kit.edu

<https://doi.org/10.36897/jme/147699>

The purpose of this article is to investigate whether it is possible to diagnose some faults in the machines by using the sensorless motor current data with the help of PLC. In general, FFT analysis is used to correlate vibration, current, sound, and acoustic signal characteristics in signal processing. Feature extraction is defined as the process of estimating some measures which will express the signal. One of the simple and fast solutions in feature extraction is statistical methods. It gives good results on uncomplicated data [5–6].

Motor current-based diagnosis has become a highly accurate and cost-effective technology. A lot of research has been carried out on motor current-based fault diagnosis, most of which is aimed at finding faults in the mechanical components of the motor. Motor internal load variations and problems (winding failures, bearing, stator, rotor failures, faults, etc.) and related mechanical component problems are contemplated. In addition, a small number of study has been made to detect problems in machines and other components using motor current data. Some of them are fault diagnosis studies of bearings [7], gears [8], linear shafts [9], misalignments and unbalances [10], oil whips [11], pumps [12], robots [13], and wind turbines [14].

Few works have been done based on the current signal for the diagnosis of linear axis misalignment. Putz et al. presented a condition monitoring system using Choi-Williams distribution [15]. Yuqing Zhou et al. established a mathematical model between motor current and machine faults [16]. In another study, Vogl et al. used data from the multi-sensor-based method, inclinometers, accelerometers, and velocity gyroscopes to find changes in linear and angular errors due to axis degradation. They compared this developed system with the laser method and the performance of this system is almost the same. No signal processing or diagnostic detection was used [17]. Reuß [18] modeled and experimentally compared the wear on linear axes and investigated the motor current. Wear on bearings and ball screws has been studied. Signal processing and intelligent fault detection algorithm were not used in this study. In general, frequency-based and time-frequency-based signal processing methods are used in studies. Using both domains enables the search for time-dependent and frequency-dependent faults alike.

In addition to these advantages, there are some disadvantages. Current signals contain fundamental and harmonic components, as well as electrical noise. These issues have to be addressed in order to efficiently extract defect-related features from the signal. Still, the fact that a new sensor is not needed for the monitoring process makes current-based machine monitoring attractive [3]. In the current state of the art, few studies are focusing on faults of linear feed axes. Hence, it is the aim of this study to investigate the potential of motor current analysis for fault detection on the linear feed axis. In this study, it was investigated whether it is possible to diagnose axial misalignment in linear feeding axes by using the motor current of the machines by FFT and Statistical methods.

## 2. THEORETICAL BACKGROUND

### 2.1. FAST FOURIER TRANSFORM (FFT)

Some signals in the time domain are not easy to find, but the characteristics after transforming to the frequency domain are easy to see [19]. For this, we use the frequency

analysis method. We can convert the signal from the time domain to the frequency domain through the Fourier transform. In order to use computers to perform Fourier transform in fields such as scientific computing and digital signal processing. The function, that is, the discrete Fourier transform, needs to be discretized. This algorithm can significantly reduce the number of multiplications required by the computer to calculate the discrete Fourier transform. In particular, the more the number of sampling points  $N$  to be transformed, the more significant the savings in calculating the FFT algorithm. In Fig. 1, the horizontal axis of the first graph is the time, vertical is the amplitude. The second graph has amplitude on the vertical axis and frequency on the horizontal axis.

## 2.2. STATISTICAL METHODS

Mean: The mean represents the DC component in the signal.

$$\mu = \frac{1}{N} \sum_{i=0}^{N-1} x_i \quad (1)$$

Root mean square: The signal is squared and then averaged to represent the average signal power. The average power of the signal is equal to the DC power of the signal plus the AC power of the signal.

$$rms = \sqrt{\frac{1}{N} \sum_{i=0}^{N-1} x_i^2} \quad (2)$$

Skewness can reflect the symmetry of the distribution.

$$K_3 = \frac{E[(X-\mu)^3]}{\sigma^3} \quad (3)$$

Kurtosis reflects the sharpness of the image.

$$K_4 = \frac{E[(X-\mu)^4]}{\sigma^4} \quad (4)$$

Wavefactor is:

$$\frac{\sqrt{\frac{1}{N} \sum_{i=0}^{N-1} x_i^2}}{\frac{1}{N} \sum_{i=0}^{N-1} x_i} \quad (5)$$

The crest factor is the ratio of the peak value of a signal to the effective value (RMS) and represents how extreme the peak value is in the waveform.

$$\frac{\max(x_i)}{\sqrt{\frac{1}{N} \sum_{i=0}^{N-1} x_i^2}} \quad (6)$$

## 3. EXPERIMENT SETUP

For this study, we used an experimental setup at the institutes' laboratory consisting of a feed drive system with a ball screw. On this experimental setup, different axial

misalignment problems can be simulated and motor current values of the VFD can be monitored at different speeds and strokes. The experimental setup consists of a ball screw mechanism, table, a fixed and loose pillow block, a workbench, a ball guide rail, the nut bracket, the linear encoder, the coupling, and a servo motor with a controller. The servo motor is from Beckhoff and the control of the test rig is realized with a Twincat PLC that provides the logic and the data acquisition capabilities. Data were collected with a sampling rate of 100. The reason for this low rate is the low sampling rate of the PLC. The signal processing is executed in Python. The experimental setup is shown in Fig. 1. In addition, the technical drawing of the experimental set is shown in Fig. 2.

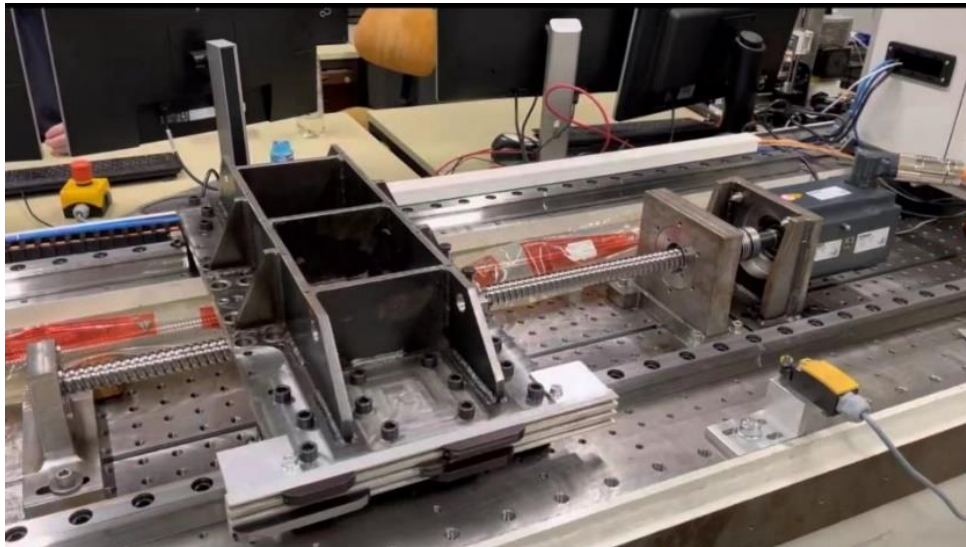


Fig. 1. Experimental setup

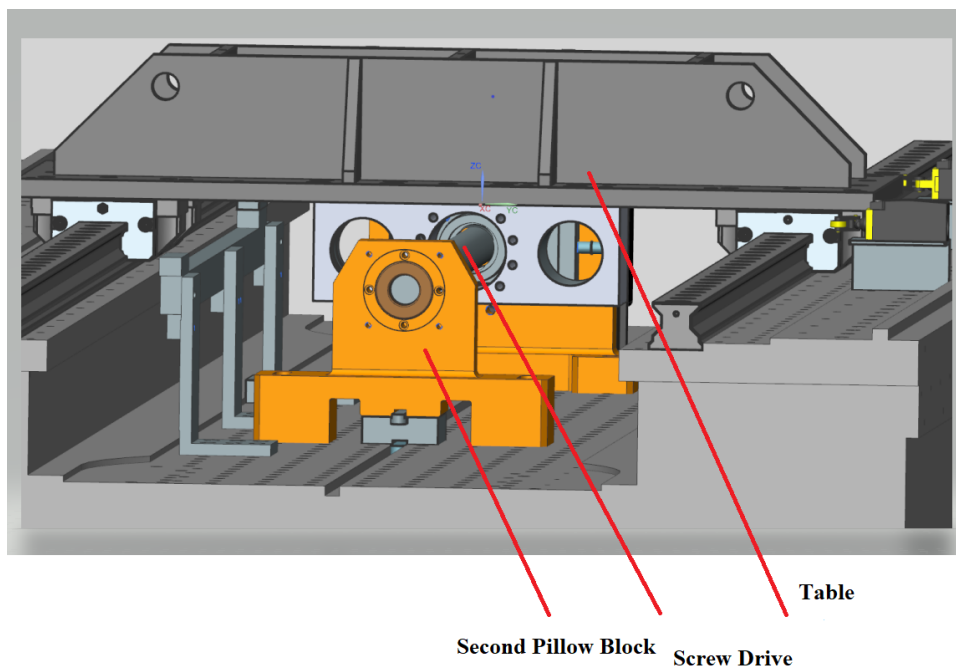


Fig. 2. Technical drawing of the experimental setup

The axial misalignment on the right side should normally give the same data as the left side. However, it has been shown that it is possible to detect misalignment in more than one pillow block. There is a right misalignment on the 1st pillow block caused by the assembly. In the second pillow block, misalignment can occur at different levels. The assembly misalignment of the 1st pillow block in the experiment set and the simulated misalignment of the 2nd pillow block is shown in Fig. 3. In this study, different stroke experiments were carried out at different speeds. In addition, different levels of axial misalignment were tested for right and left axial misalignment. Each experiment was repeated 25 times for the diagnostic algorithms to be used in the future. It was observed that all of the repetitions were similar. In this study, 0.5 and 1 mm axial misalignment are included. The velocity values of 100 and 200 mm/s were used by keeping the stroke value constant.

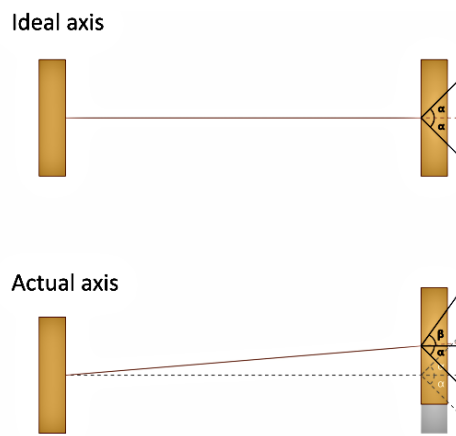


Fig. 3. Explanation of axial misalignment in the experimental set

The normal state left misalignment, right misalignment states are simulated in the linear feeding axis. After trying many different strokes, a 100 mm stroke was chosen depending on the sampling rate of the PLC. Experiments were made at speeds of 100 and 200 mm/s. Experiments were carried out at 0.5 and 1 mm levels for left and right axis misalignment. These axial misalignments are simulated with the number 2 pillow block. In addition, there is a permanent right axis misalignment in the number 1 pillow block due to assembly. Each experiment was repeated 25 times. The experiment plan is given in Table 1.

Table 1. Experiment plan

Stroke	Speed	Misalignment situation	Repeat times
100 mm	100 mm/s	Normal condition	25
		Left misalignment 0.5 mm	25
		Left misalignment 1 mm	25
		Right misalignment 0.5 mm	25
		Right misalignment 1 mm	25
		200 mm/s	200 mm/s
Left misalignment 0.5 mm	25		
Left misalignment 1 mm	25		
Right misalignment 0.5 mm	25		
Right misalignment 1 mm	25		

#### 4. RESULT

The time variation of the motor current signals obtained in different situations is investigated. When the comparison is made in Fig. 4. It can be seen from the signals that the amplitude values increase when an axial misalignment was applied. Signal processing is done with an FFT to convert from time-domain signals to frequency domain signals and analyze the differences. The stroke of this experiment is 100 mm (from absolute position 400 mm to 500 mm) and has a table speed of 100 mm/s (600 rpm). The unit given as rpm is the rotational speed of the motor that moves the table. In the axis misalignment problem, there is an increase in the second and third peak amplitude values in the FFT. The stroke frequency of the table and its reflections come out at different points due to the sampling rate of the PLC, the table waiting at the start and endpoints.

Due to the friction effect between the axis and the table, the values related to the friction increase as the left axis misalignment increases in the 2<sup>nd</sup> pillow block in the FFT and Statistical method. Normally, the same trend should be in the right axis misalignment. Since there is a right axis misalignment in the 1<sup>st</sup> pillow block, which is fixed in our experimental set, the values decrease at the beginning when the 2<sup>nd</sup> pillow block has a right axis misalignment, and then increase again after reaching a certain value. If there was a fixed left axis misalignment in the 1<sup>st</sup> pillow block, the values would decrease as the left axis misalignment increased in the 2<sup>nd</sup> pillow block, and then increase again after a certain value. If the 1<sup>st</sup> bearing had been placed properly, the values would have increased in the right and left axis misalignments.

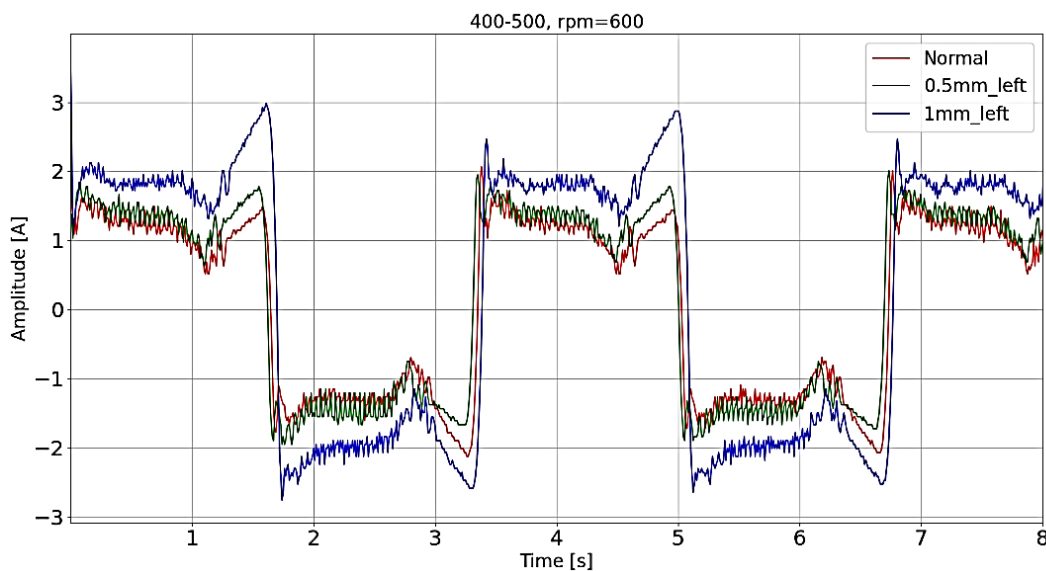


Fig. 4. The current value of servomotor (Table speed:100 mm/s, Stroke:100mm)

The current values transmitted from the FFT are shown in Fig. 5. The  $x$ -axis in the figure represents the frequency, and the  $y$ -axis represents the corresponding amplitude. The plot shows that the value of the amplitude increases significantly for different axis misalignments.

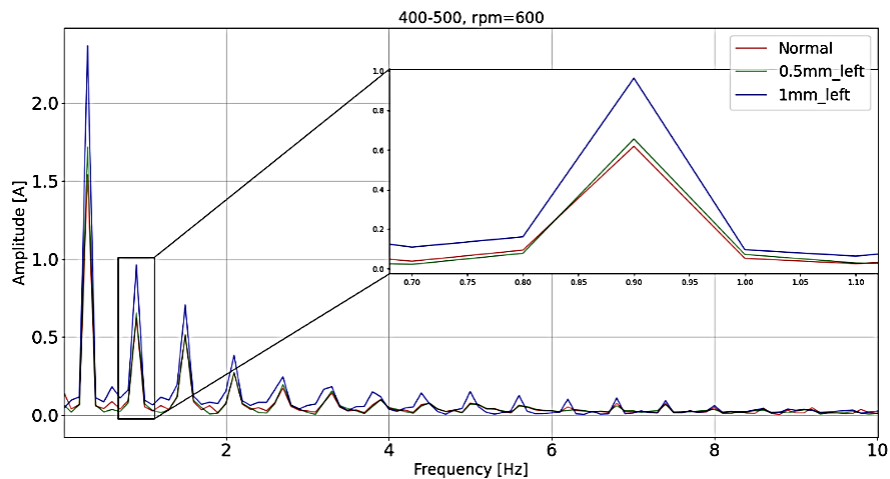


Fig. 5. The current values in frequency-domain (Table speed:100 mm/s, Stroke:100mm)

Also, the amplitude in the frequency domain increases with axial misalignment. Several experiments were conducted to confirm, whether this phenomenon is reproducible and the same conclusion was reached. Figure 6 shows different speeds in the same stroke. The table moves at 200 mm/s. If the change in signals in the time domain is compared, although the trend of the current signal is the same, the amplitude value changes. It can be seen more clearly when analyzed in the frequency domain with the FFT in Fig. 7. As seen in the figure, there is no change in frequency, but the amplitude value changes depending on the axial misalignment. The amplitude value increases in the left axis misalignment and decreases in the right axis misalignment. Although the table speed has been doubled, the main frequency and reflections have increased from 0.9 to 1.1. This is because the table waits at the start and endpoints and the data sampling is low in the PLC. Therefore, the frequency change does not increase proportionally. However, the axis misalignment problem can be clearly identified from here.

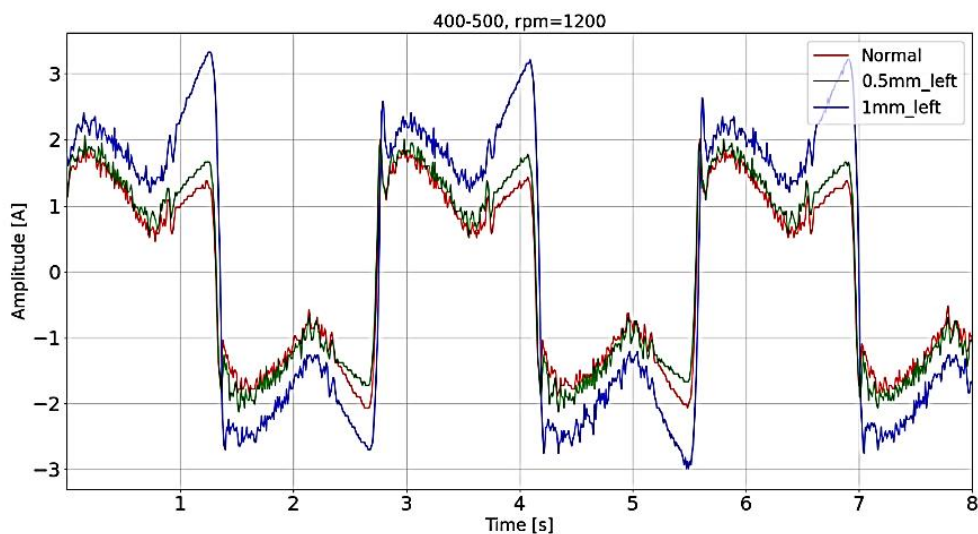


Fig. 6. The current value of servomotor (Table speed:200 mm/s, Stroke:100 mm)

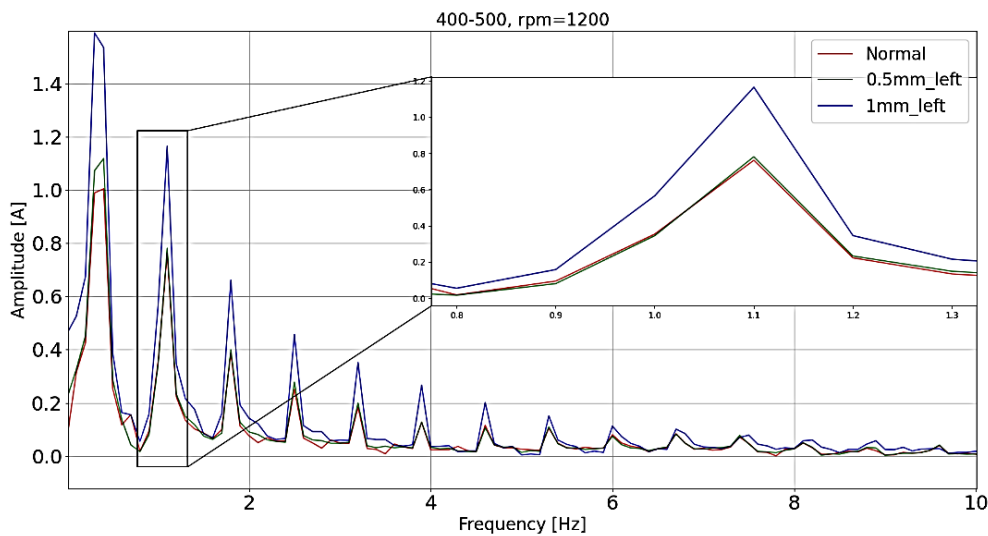


Fig. 7. The current values in frequency-domain (Table speed: 200 mm/s, Stroke: 100 mm)

As a result of different experiments, it was seen that left side axis misalignment could be detected at different speeds and the amplitude-frequency changed. In case of axial misalignment in the right direction, the table is fixed with two pillow blocks of bearing. Axis misalignment is made from the second pillow blocks of bearing where the end stroke is. The bed at the beginning is fixed. During assembly, there is a right axial misalignment on this pillow block. When axial misalignment is simulated to the right, the gap gets smaller up to a point and therefore the amplitude value decreases. Then it goes up again. When 0.5 mm axial misalignment is given, the amplitude value gets smaller because the gap gets smaller, then when 1 mm was applied, the gap value starts to grow as it gets larger again. With this method, it is possible to detect more than one axis misalignment. This change is shown in Figs. 8–11.

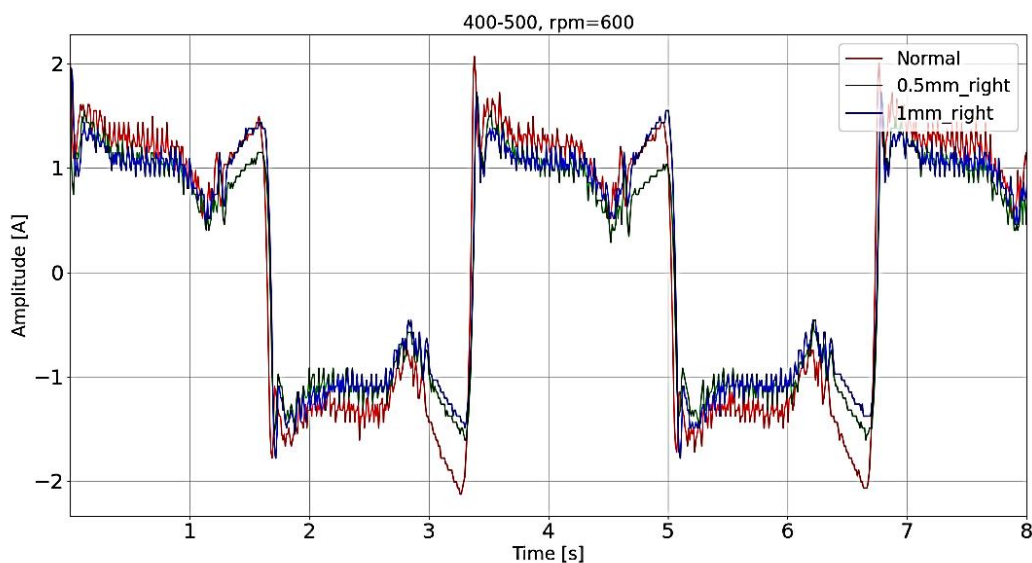


Fig. 8. The current value of servomotor (Table speed: 100 mm/s, Stroke: 100 mm)

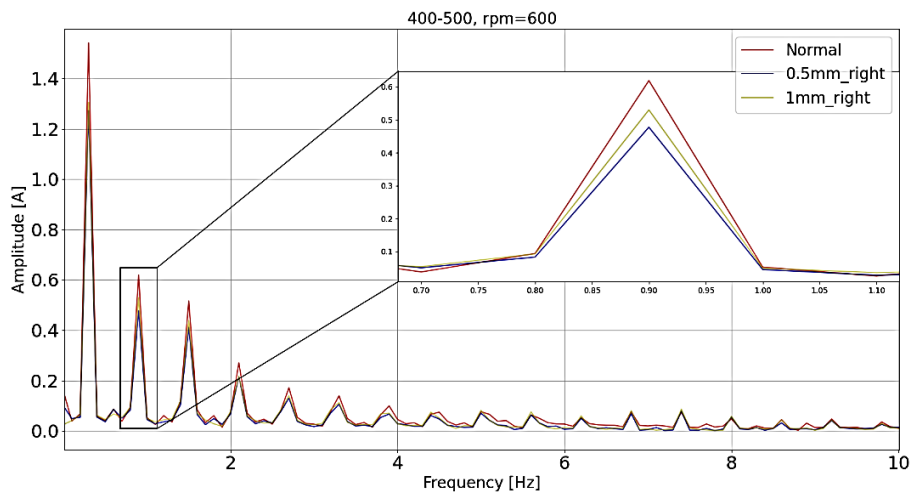


Fig. 9. The current values in frequency-domain (Table speed:100 mm/s, Stroke:100 mm).

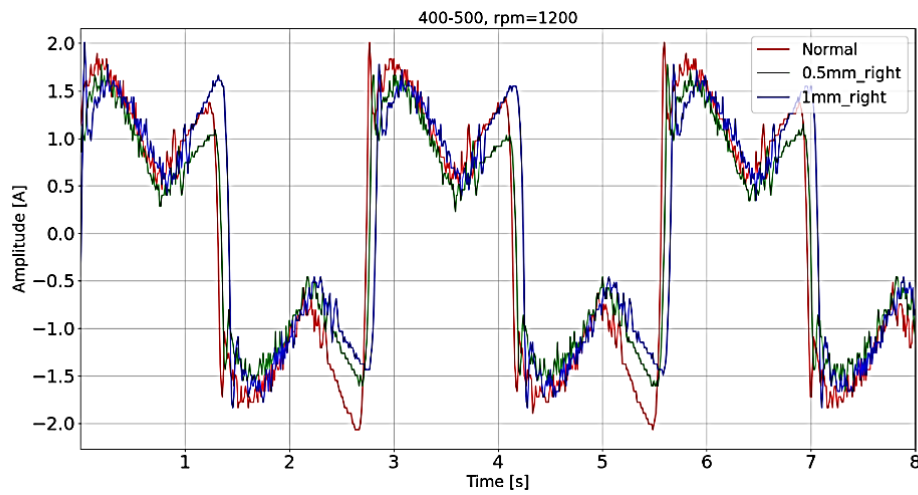


Fig. 10. The current value of servomotor (Table speed:200 mm/s, Stroke:100 mm)

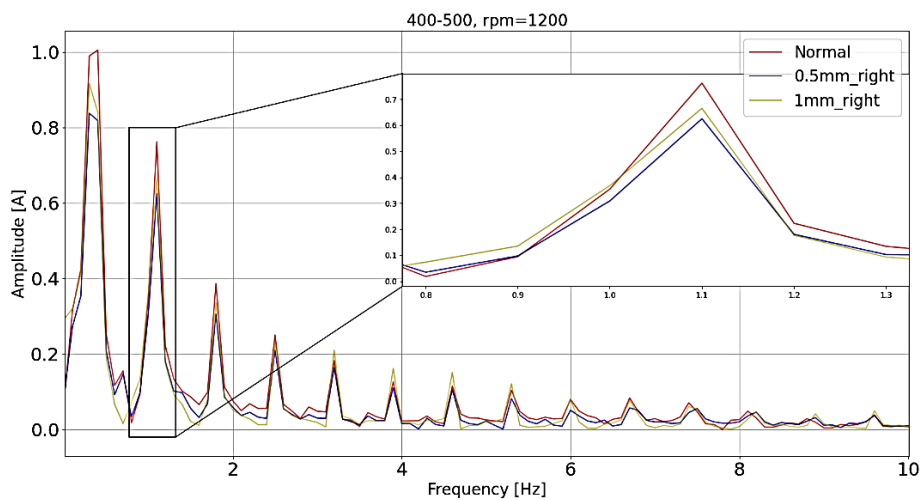


Fig. 11. The current values in frequency-domain (Table speed:200 mm/s,Stroke:100 mm)

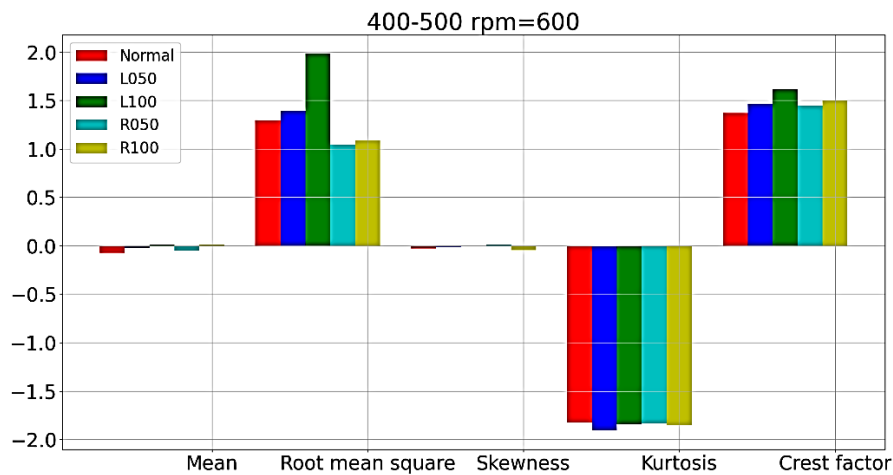


Fig. 12. Statistical results at 100 mm/s and 100 mm stroke

When the results are analyzed statistically, mean and root-mean-square values increase as the left axis misalignment gets larger. Other statistical methods do not give a significant result. In the right axis misalignment, the values decrease at 0.5 mm and increase again when it is 1 mm. Statistical results are shown in Figs. 12 and 13.

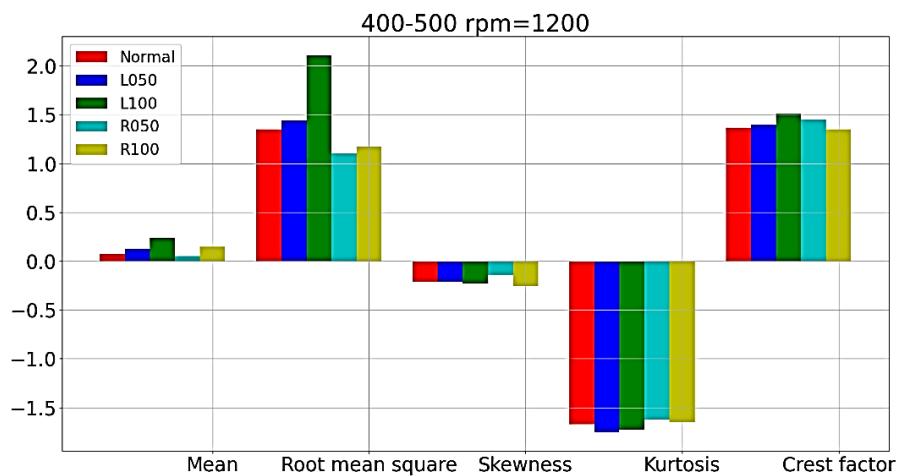


Fig. 13. Statistical results at 200 mm/s and 100 mm stroke

## 5. CONCLUSION AND FUTURE WORKS

In the study, it is seen that as the axial misalignment increases, the FFT amplitude value and statistical results increase in the left axis misalignment. It was observed that the right axis misalignment decreased up to 0.5 and then increased. It was concluded that the reason for this was due to the assembly error and more than one axis misalignment could be detected. From the results, it is seen that it is possible to monitor and diagnose axial misalignment errors of linear feed axes by using the servo motor current data obtained from PLCs, and research

on this subject should continue. But when we apply this to real systems, the time-dependent signal changes depending on the environmental conditions. This causes incorrect fault diagnosis. The FFT-based approach is less affected at this point. In this system, frequency-based and time-based signal processing techniques should be used together in fault diagnosis using the frequency and amplitude values of the peaks in FFT and statistical results to find the problem by comparing the differences between these values. Since each machine has a motor and they are controlled by a PLC or NC, there is no need to install additional sensors, decreasing time and money spent on the machinery. With this approach, current diagnostics and monitoring of feed axes can become more available in the industry. In addition, It is possible to make automatic fault diagnoses by classifying the results obtained in this study with different machine learning methods in the future [20–21]. In addition to these, In our studies, it is seen that weight changes do not affect the results, but force changes do. In addition, vertical axis misalignments will also be investigated. These results will be shared in future studies.

The effect of force change and weight change on motor current data will be discussed in later studies. The behavior of the motor current against the force and weight change at different levels will be examined. Accordingly, the deep learning algorithm will be trained. In addition to these, the most ideal speed stroke values will be determined for the fault diagnosis of the table.

As a result, automatic detection of equipment malfunctions is possible using motor current and it is possible to use this sensorless method in diagnosing problems of other machine parts.

#### REFERENCES

- [1] VOGL G.W., CALAMARI M., YE S., DONMEZ M.A., 2016, *A Sensor-Based Method for Diagnostics of Geometric Performance of Machine Tool Linear Axes*, *Procedia Manufacturing*, 5, 621–633.
- [2] ALTINTAS Y., VERL A., BRECHER C., URIARTE L., PRITSCHOW G., 2011, *Machine Tool Feed Drives*, *CIRP Annals*, 60/2, 779–796.
- [3] LEITE V.C.M.N., DA SILVA J.G.B., TORRES G.L., VELOSO G.F.C., DA SILVA L.E.B., BONALDI E.L., DE OLIVERIA L.E.D.L., 2017, *Bearing Fault Detection in Induction Machine Using Squared Envelope Analysis of Stator Current*, *Bearing Technology*, London, UK: InTech., DOI: 10.5772/67145.
- [4] VOGL G.W., DONMEZ M.A., ARCHENTI A., 2016, *Diagnostics for Geometric Performance of Machine Tool Linear Axes*, *CIRP Annals*, 65/1, 377–380.
- [5] CIABATTONI L., FERRACUTI F., FREDDI A., MONTERIU A., 2017, *Statistical Spectral Analysis for Fault Diagnosis of Rotating Machines*, *IEEE Transactions on Industrial Electronics*, 65/5, 4301–4310.
- [6] YU X., DONG F., DING E., WU S., FAN C., 2017, *Rolling Bearing Fault Diagnosis Using Modified LFDA and EMD with Sensitive Feature Selection*, *IEEE Access*, 6, 3715–3730.
- [7] HOANG D.T., KANG H.J., 2019, *A Motor Current Signal-Based Bearing Fault Diagnosis Using Deep Learning and Information Fusion*, *IEEE Transactions on Instrumentation and Measurement*, 69/6, 3325–3333.
- [8] MOHANTY A.R., KAR C., 2006, *Fault Detection in a Multistage Gearbox by Demodulation of Motor Current Waveform*, *IEEE Transactions on Industrial Electronics*, 53/4, 1285–1297.
- [9] PUTZ M., TRIMBORN C., NAUMANN C., FISCHER J., NAUMANN M., GEBEL L., 2018, *Sensorless Fault Detection in Linear axes with Dynamic Load Profiles*, *Procedia Manufacturing*, 19, 66–73.
- [10] VERMA A.K., SARANGI S., KOLEKAR M.H., 2013, *Misalignment Fault Detection in Induction Motor Using Rotor Shaft Vibration and Stator Current Signature Analysis*, *International Journal of Mechatronics and Manufacturing Systems*, 6/5–6, 422–436.
- [11] ALOK K.V., SOMNATH S., MAHESH K., SHREYA B., 2012, *Oil Whip Detection Using Stator Current Monitoring*, *IEEE Symposium on Computers & Informatics (ISCI)*, IEEE, 119–124.
- [12] PRADHAN P.K., ROY S.K., MOHANTY A.R., 2020, *Detection of Broken Impeller in Submersible Pump by Estimation of Rotational Frequency from Motor Current Signal*, *Journal of Vibration Engineering & Technologies*, 8, 613–620.

- [13] YANG Q., LI X., WANG Y., AINAPURE A., LEE J., 2020, *Fault Diagnosis of Ball Screw in Industrial Robots Using Non-Stationary Motor Current Signals*, *Procedia Manufacturing*, 48, 1102–1108.
- [14] DAHIYA R., 2018, *Condition Monitoring of Wind Turbine for Rotor Fault Detection Under Non Stationary Conditions*, *Ain Shams Engineering Journal*, 9/4, 2441–2452.
- [15] PUTZ M., TRIMBORN C., NAUMANN C., FISCHER J., NAUMANN M., GEBEL L., 2018, *Sensorless Fault Detection in Linear axes with Dynamic Load Profiles*, *Procedia Manufacturing*, 19, 66–73.
- [16] ZHOU Y., MEI X., ZHANG Y., JIANG G., SUN N., 2009, *Current-Based Feed axis Condition Monitoring and Fault Diagnosis*, 4th IEEE Conference on Industrial Electronics and Applications, IEEE, 1191–1195.
- [17] VOGL G.W., CALAMARI M., YE S., DONMEZ M.A., 2016, *A Sensor-Based Method for Diagnostics of Geometric Performance of Machine Tool Linear Axes*, *Procedia Manufacturing*, 5, 621–633.
- [18] REUß M., 2017, *Modeling Method for Simulation of Assembly Variances*, Stuttgart University, Phd Thesis, Stuttgart, Fraunhofer Verlag.
- [19] WU Z., JIANG H., ZHAO K., LI X., 2020, *An Adaptive Deep Transfer Learning Method for Bearing Fault Diagnosis*, *Measurement*, 151, 107227.
- [20] MOURTZIS D., 2021, *Towards the 5th Industrial Revolution: a Literature Review and a Framework for Process Optimization Based on Big Data Analytics and Semantics*, *Journal of Machine Engineering*, 21/3, 5–39.
- [21] PUTNIK G.D., SHAH V., PUTNIK Z., FERREIRA L., 2021, *Machine Learning in Cyber-Physical Systems and Manufacturing Singularity—it Does not Mean Total Automation, Human is Still in the Centre: Part II—In-CPS and a View from Community on Industry 4.0 Impact on Society*, *Journal of Machine Engineering*, 21/1, 133–153.